CRYOBIOLOGY **33,** 472–482 (1996)
ARTICLE NO. 0048

An Experimental Study of the Mechanical Response of Frozen Biological Tissues at Cryogenic Temperatures

YOED RABIN,*,† PAUL S. STEIF,* MICHAEL J. TAYLOR,‡ THOMAS B. JULIAN,† AND NORMAN WOLMARK†

**Department of Mechanical Engineering, Carnegie Mellon University, 5000 Forbes Avenue, Pittsburgh, Pennsylvania 15213-3890; and ‡Cryobiology Research Program and †Division of Surgical Oncology, Allegheny General Hospital, Medical College of Pennsylvania and Hahnemann University, 320 East North Avenue, Pittsburgh, Pennsylvania 15212-4772*

An experimental study of the mechanical response of frozen soft biological tissues to applied compressive stresses is presented. This study is related to the mechanical stresses that develop due to the contraction of frozen tissues in cryopreservation as well as in cryosurgical procedures. The main concept in this study is that the stresses associated with the constrained contraction of the frozen tissue, i.e., due to temperature variations within the frozen tissue, can be simulated by an external mechanical load which is applied to the frozen tissue while the tissue is maintained at a uniform temperature. A new apparatus for measuring compressive stresses and strains of frozen biological tissues in cryogenic temperature range is presented. A new technique for processing the fresh biological tissue into a cylindrical frozen sample for mechanical testing is introduced. Results of compression tests on rabbit liver, kidney, and brain are presented and are compared with available data from the literature on sea ice and single ice crystals. An unusual response of frozen biological tissues to compressive stress was observed: after the initial, roughly linear elastic portion there was a series of sudden stress drops at constant strain, each followed by a linear increase of stress with strain to the next drop. This phenomenon, which is attributed to the accumulation of microcracks, broadly resembles plastic deformation, and thus provides some support for simple mechanical models invoked in theoretical studies. © 1996 Academic Press, Inc.

The extent of injury of biological tissues by freezing is influenced by many factors: the cooling rate (5, 7, 23), the thawing rate (17), the minimal temperature achieved (6), the number of repeated freezing–thawing cycles (8, 20), and the presence of cryoprotectants (4, 22). The mechanisms of cryodestruction may generally be separated into two groups: the first is related to the freezing process within the phase transition temperature range (0 to −22°C), while the second group is related to further destruction after phase transition has completed. Destruction mechanisms of the first group are related to heat transfer, mass transfer, and chemical equilibrium in the intracellular and extracellular solutions (13–16). Mechanical interaction between ice crystals and cells also affects the destruction process during the phase transition process (11).

Destruction mechanisms after the phase transition has been completed are related to thermal stresses in the frozen state. It has been suggested that elastic deformations resulting from these stresses may cause mechanical damage to cell membranes (21). High thermal stresses may develop due to large temperature differences at the frozen region, as is the case in a typical cryosurgical procedure (19), or in the process of cryopreservation (5, 10). It was demonstrated theoretically that, for a spherical cryoprobe and typical physical properties of ice, the thermal stress can easily reach the yield strength of the frozen tissue (19). It was proposed that thermal stresses which produce plastic (permanent) deformation of the frozen tissue may therefore severely increase the mechanical damage to the cell's mem-

Received April 23, 1996; accepted June 4, 1996.

0011-2240/96 $18.00
Copyright © 1996 by Academic Press, Inc.
All rights of reproduction in any form reserved.

brane and to the tissue structure. The analysis accounted for plastic deformations by assuming an elastic–perfectly plastic model for the mechanical response of the freezing tissue. However, this idealized response to a mechanical load has not been based on experimental data since, to the best of our knowledge, such data have not been reported. The analysis in Ref. (19) revealed that both tensile and compressive stress exist in a cryoprocedure. Hence, both tensile and compressive strength are of interest.

The aim of the present experimental study was to examine the response of the frozen soft biological tissues to compression under an external load. The main concept underlying this study is that the stresses associated with the constrained contraction of the frozen tissue, i.e., due to temperature variations within the frozen tissue, can be simulated by an external mechanical load which is applied to the frozen tissue while it is maintained at a uniform temperature. The rationale for this concept is well established in the study of deformable bodies: the deformations associated with stresses are not dependent on the origin of the stress. The response of the frozen tissue to an external load is a function of many factors such as the percentage of blood and other body fluids per unit volume of tissue, chemical content, properties of the extracellular matrix, and fiber strength and orientation. The mechanical properties under study in the present work are the yield strength, the maximal strength, and the elasticity modulus, where the ratio of the tissue strength to its elasticity modulus is the most important parameter in an elastic–perfectly plastic model (19).

A new apparatus for measuring the stress–strain relationship in a frozen biological tissue, in a cryogenic temperature range, is described. The apparatus is based on a standard load device and a special load chamber for low temperatures. A new technique for processing the fresh biological tissue into a cylindrical frozen sample for a compression load test is introduced. Results of compression tests on rabbit liver, kidney, and brain are presented and are compared with available data from the literature on sea ice and single ice crystals.

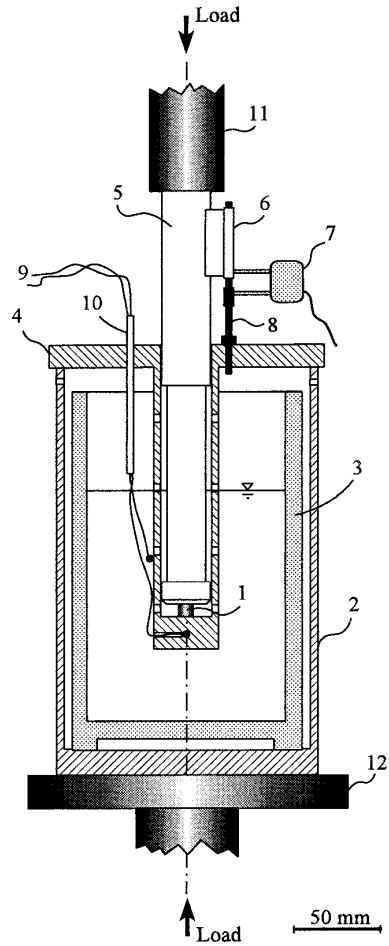

FIG. 1. Schematic presentation of the load chamber of the experimental apparatus for compression tests of frozen tissues in cryogenic temperatures. See text for details.

EXPERIMENTAL SETUP

The experimental apparatus is based on a standard mechanical testing system: MTS-976.21-23. The load is applied by an hydraulic piston, with accurate control of the rate of loading. The load magnitude is measured by a load cell MTS-661.21A-03. As illustrated in Fig. 1, a special loading chamber has been

designed and constructed to accommodate the frozen tissue sample during the tests. In order to maintain a constant cryogenic temperature, the tissue sample was immersed in liquid nitrogen while the experiment was performed.

All parts of the loading chamber were made of commercial steel, unless otherwise noted. With reference to Fig. 1, the load-carrying components of the chamber are: shell 2, which rests on ram 12; cover 4, which rests on the shell, consisting of an annular disk to which is welded a capped tube; and column 5, which presses against the stationary platen 11 on its upper end and bears on the tissue sample 1 on its lower end. Hence, if the steel components are viewed as essentially rigid, then the upper face of the tissue sample 1 is held stationary, while its lower face displaces upward with the tube cap, tube, disk, and shell which are rigidly driven by the ram 12.

Shell 2 has the following dimensions: a height of 235 mm, an outer diameter of 140 mm, a wall thickness of 6.35 mm, and a base thickness of 12.7 mm. Four holes, each 5 mm in diameter, were drilled in shell 2, at a distance of 16 mm from the shell edge to relieve nitrogen gas. The vacuum insulated container 3 is stainless steel (Thermos) and holds up to 0.75 liters of coolant. The annular disk has an outer diameter of 150 mm, an inner diameter of 25.4 mm, and a thickness of 12.7 mm; the tube has an outer diameter of 32 mm, an inner diameter of 25.4 mm, and a length of 175 mm, which includes the 19-mm-thick cap. Eight equally spaced holes, each 3 mm in diameter, were drilled along the tube, four on each side, to allow the liquid nitrogen to surround the tissue sample. Column 5 has a total length of 240 mm. The upper 112 mm and bottom 13 mm have a diameter of 25.35 mm allowing smooth, yet constrained axial movement relative to the annular disk and tube. The column has a reduced diameter of 20.6 over the remaining 115 mm; this reduces friction between the column and the tube and permits liquid nitrogen to flow freely inside the tube.

The displacement of cover 4 (which essentially moves with the lower surface of the tissue sample) relative to column 5 (which keeps the upper surface of the tissue sample stationary) is measured by extensometer 7, MTS-632.110-20. One arm of the extensometer is connected to column 5 by fixture 6, while the other arm is connected to disk 4 by rod 8. A hole in fixture 6 acts a guide for the upper end of rod 8.

Temperatures were monitored at two points by copper–constantan thermocouples, 9. One thermocouple was located at the center of the cap of cover 4 through a 1-mm hole, while the other was attached to the tube, above the tissue's upper surface. The second thermocouple served as a liquid nitrogen level indicator; it shows the liquid nitrogen boiling temperature as long as the sensor is below the coolant level.

METHOD OF OPERATION

Tissues to be used in the compression tests were obtained from 12 New Zealand White rabbits (2.5–4 kg) by excising the liver, kidneys, and brain soon after death. These organs were procured from rabbits that had been sacrificed for other studies in which the heart was excised under general anesthesia of halothane (2.5 liters/min) administered via a ventilator. These procedures were carried out in accordance with the guidelines and standards of the United States Public Health Services for use and care of laboratory animals and with the approval of the Institutional Animal Care and Use Committee of the Allegheny-Singer Research Institute.

Compression tests were performed on frozen cylindrical tissue samples of rabbit liver, kidney, and brain. Tissue samples were taken immediately after the animal was sacrificed according to the following protocol. The fresh organ, i.e., liver, kidney, or brain, was excised from the body and placed on a flat dish. The dish was sealed and placed immediately in a freezer, maintained at −20°C, for a period of 48 to 72 h. The sealing was required in order to avoid drying of the tissue surface. Special

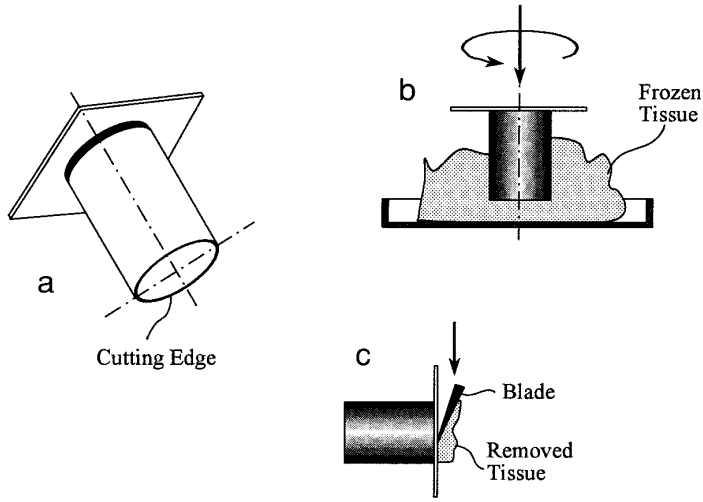

FIG. 2. Schematic presentation of a cutting tool (a) for the preparation of a cylindrical sample of a frozen tissue and its way of operation. First, the cutting tool cuts a cylinder of frozen tissue (b) and then the bases of the cylinder are cut perpendicular to the cylinder centerline (c).

care was taken to avoid blood losses from the organ (especially in the liver case). Using a cylindrical cutting tool (Fig. 2a), cylindrical samples were cut out from the frozen organs (Fig. 2b). Using a sharp blade, the bases of the cylindrical sample were cut perpendicular to the centerline of the cylinder (Fig. 2c). Cutting and shaping the tissue sample was accomplished in a few minutes, without any significant thawing of the frozen organ. The shaped cylindrical sample was than immersed immediately in liquid nitrogen and kept at −196°C until the compression test was performed, a day or two later. Cutting tools having an inner diameter of 8.7 and 11.8 mm were used. The ratio of the height to the diameter of each sample was kept in the range of 0.8 to 1.5.

Prior to experimentation shell 2 (Fig. 1) was placed on the load device, and container 3 was placed inside the shell and filled with liquid nitrogen. The tube of cover 4 and column 5 were precooled for a few minutes. The tissue sample was transferred in the frozen state and placed on the upper surface of the cap of the tube. The column was inserted into the tube so that rod 8 slides into fixture 6. Cover 4 was placed on shell 2, while the tissue sample, together with a part of the column and a part of the tube, was immersed in the liquid nitrogen. Finally, the extensometer arms were connected by rubber bands to fixture 6 and rod 8.

The experiment was started after all parts reached thermal equilibrium. The thermal equilibrium was observed as the extensometer signals decay, i.e., no relative movement was observed between the cover and the beam. It was noted that the extensometer movement can be observed long after the thermocouples are showing a constant temperature. Finally, the test was performed under displacement control, with a velocity of 0.083 mm/min. The values of load vs the relative displacement at the extensometer were plotted and the thermocouple temperatures were monitored. The precooling period took about 15 min for the first test and between 2 and 3 min between each two successive tests. Each compression test took from 3 to 10 min depending on the dimensions of the frozen sample, the tissue type, and the number of the load cycles.

Pilot tests were performed, with and without tissue samples, to study the load chamber

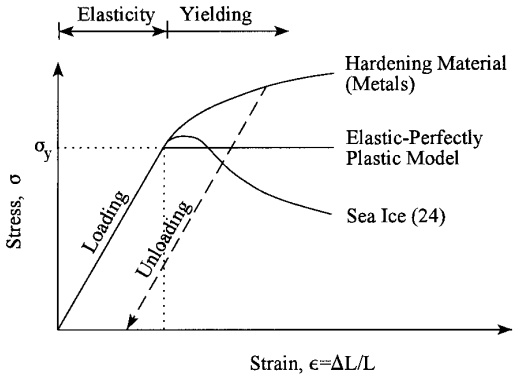

FIG. 3. Schematic presentation of typical stress–strain relationships for various materials.

response. Displacements measured with tissue samples were more than two orders of magnitude larger than the displacements of the load chamber without tissue samples. Therefore, the load chamber is sufficiently rigid relative to the tissue that it can be neglected in analysis of the data.

RESULTS AND DISCUSSION

The mechanical response of materials is typically plotted in terms of stress σ (axial force divided by specimen cross-sectional area) versus strain ϵ (change in length of specimen divided by initial length). To put the stress–strain curves of frozen tissues in context, two schematic stress–strain curves (measured in compression) of other materials are shown in Fig. 3. Metals (the most widely studied materials) typically have an initial linear portion referred to as the elastic regime; the slope is the elastic modulus E (or Young's modulus). In this regime, the strain will decrease to zero again if the load (and hence stress) were to be reduced to zero. At a certain point, the stress–strain curve becomes nonlinear and assumes a slope which is markedly lower than that in the elastic regime. This is referred to as the plastic regime, and the point at which noticeable deviations from linearity occur is called the yield stress, σ_y. In metals, the underlying mechanism of deformation changes from one of stretching of interatomic bonds to one of crystal planes slipping over one another through the movement of dislocations, which are defects in the crystalline lattice. Hardening denotes the tendency for the stress to drive this second deformation mechanism to increase as the strain increases; materials vary widely as to their rate of hardening (the slope of the strain–stress curve in the plastic regime). This regime of deformation is referred to as plastic for the following reason. When the sample is unloaded (the stress reduced), the dashed stress–strain curve in Fig. 3 is followed, rather than original stress–strain curve; there remains a permanent plastic strain after the stress has been reduced completely to zero. This general stress–strain response is typical for metals. A stress–strain curve for sea ice is also shown in Fig. 3 (24).

A simplified elastic–perfectly plastic model, representing idealized plastic behavior, is also shown in Fig. 3. The only difference between this and a more realistic curve, such as of metal or of sea ice, is the sudden change from the elastic slope to a flat curve with zero slope (no hardening). This model still reflects the permanent deformation that remains upon unloading. It should also be noted that in this model (and to a good approximation in actual stress–strain curves) reloading of the sample involves retracing the dashed unloading curve with plastic deformation resuming when the original plastic curve is reached.

A representative stress–strain curve for liver tissue is presented in Fig. 4. The ram moves steadily (and hence the strain increases steadily) from the beginning to the end of the test. Following a roughly linear regime, the stress suddenly drops. Since displacement is controlled, the stress drop represents a sudden drop in the material's load-carrying capacity. The stress then increases to a somewhat higher level at which point an additional stress drop occurs. After some number of stress drops (each generally at an increasingly higher level of stress), a maximum stress is reached; this point is designated by M in Fig. 4. For many

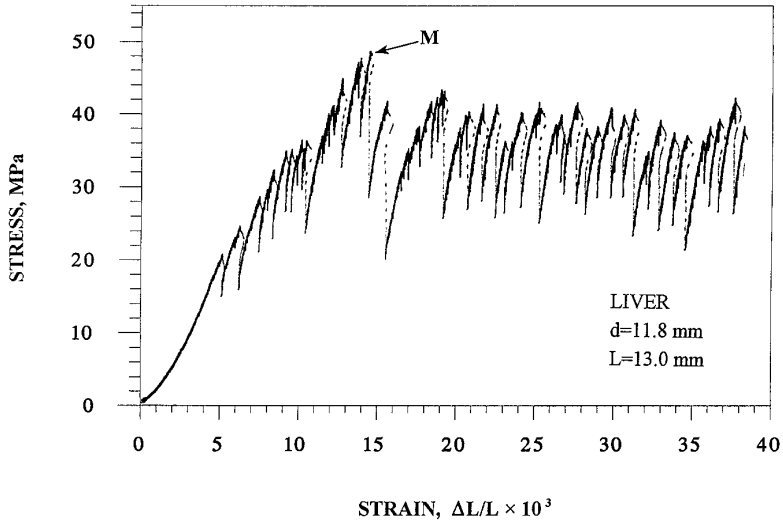

FIG. 4. Typical results of a load test of a liver sample.

of the samples, the following additional observation was made: at some strain after the maximum stress is reached, the stress drops assume a sawtooth pattern, with the maximum and minimum stresses being approximately constant. Eventually, the sample reaches a strain at which complete failure occurs, with the specimen reduced to rubble.

Some compression tests were performed in which the sample was unloaded at several points prior to final failure (Fig. 5). The first unloading sequence from B to C essentially followed the initial portion AB, suggesting that the material is indeed still elastic at B. The load is raised again and at point E the first stress drop occurs. The stress at E might be termed the yield stress. Thereafter, under constantly increasing strain, a series of stress drops occur, and then at F the sample was fully unloaded to G, leaving some permanent strain. Clearly, upon unloading, the shape of the stress–strain curve is similar to the initial elastic curve. Upon reloading, no stress drops occurred until the point I, which is at a stress similar to that at which previous load drops occurred. Load drops continued to occur under steadily increasing strain until total failure at J.

To summarize the observations, we have found elastic behavior up to rather small strains, on the order of 0.005, and a sawtooth pattern of stress thereafter featuring a series of sudden stress drops followed by a linear return to a roughly constant upper level of stress. The stress drops are on the order of one-third to one-half of the upper level of stress. The linear returns to the upper stress level occur with a slope that is close to the initial slope, although, after considering the statistics of the 26 samples, there appears to be on average a 10% *increase* in slope between the initial slope and the final slope to failure. At any point the stress can be reduced to zero leaving a permanent strain; reloading brings the stress linearly up to the upper level of stress at which point the stress drop phenomenon reappears. Final failure occurs at relatively large strains, 10 times that at which the first stress drop appears, reducing the specimen to rubble.

Certainly, in detail the observations differ sharply from the smooth curve of a plastically deforming metal. One is tempted to speculate that the stress drops correspond to the formation of small fissures or microcracks in the

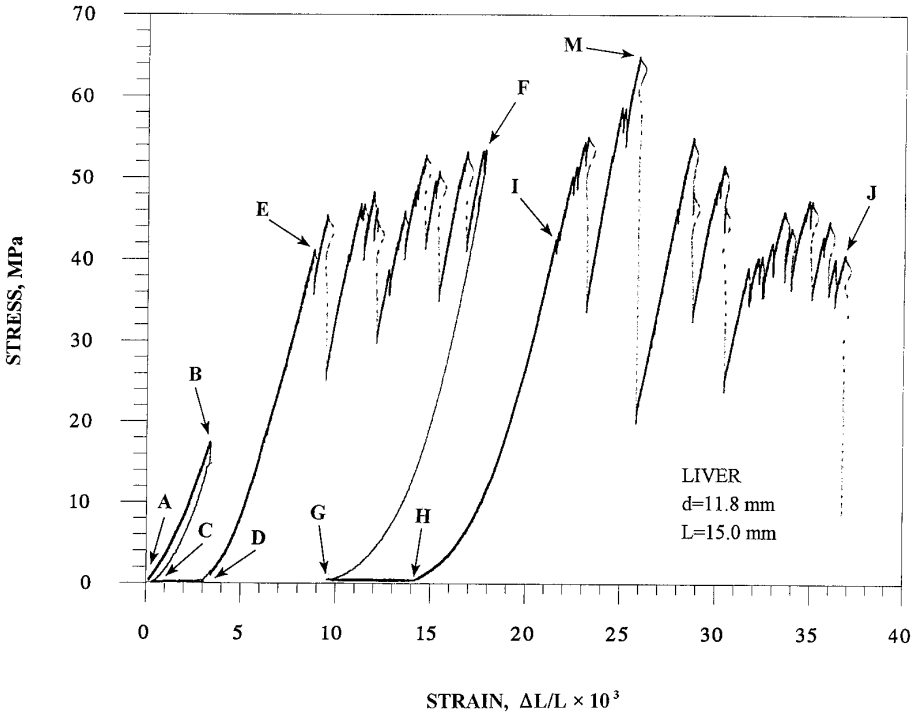

FIG. 5. A demonstration of a multiload cycle.

material. However, these cracks do not propagate very far after initiating (as indicated by the continuing ability to carry load), perhaps because they encounter internal boundaries which arrest them. Such a phenomenon is not uncommon in heterogeneous brittle materials. Normally, one would expect the slope of the stress–strain curve to drop after microcracks initiate (18). Hence, the return to roughly the original elastic slope suggests partial ''healing'' at the cracks, where the term healing is used in the sense that the specimen has a renewed ability to carry load but not in the sense that the microcracks have disappeared. That there should be a gradual increase in slope with increasing microcracks is curious and remains unexplained. The final and sudden reduction of the sample to rubble at complete failure is suggestive of a solid riddled with microcracks which reaches some critical point at which all the cracks coalesce.

On the other hand, when the results are viewed broadly, they are reminiscent of an elastic–perfectly solid in that there is an elastic portion followed by a region in which continued deformation can occur at roughly constant stress. The continuing deformation is plastic in the sense that unloading of the specimen leaves it with a permanent strain; smooth reloading up to the previous level can take place at which point continuing ''plastic'' deformation can occur.

However, defining an average stress at which continuing plastic deformation can occur is not simple given the nonsmooth nature of the stress–strain curves. The stress at which the first stress drop occurs is quite erratic, sometimes being very low. Thereafter, though, one typically sees an isolated strain at which a maximum stress is reached, while during the remainder of the strain history, the stress fluctuates between roughly consistent levels.

TABLE 1
Experimental Data of Elasticity Modulus and Strength of Rabbit Liver, Kidney, and Brain, Compared with Mechanical Properties of Single Ice Crystals and Sea Ice

Material	Elasticity modulus (mean ± STD) GPA	Yield strength (mean ± STD) MPa	Maximal strength (mean ± STD) MPa	Reference
Rabbit liver	14.8 ± 4.5 (n = 26)		53.5 ± 9.1 (n = 11)	Present study
Rabbit kidney	22.9 ± 4.6 (n = 30)		132.2 ± 35.1 (n = 11)	Present study
Rabbit brain	9.5 ± 1.7 (n = 7)		29.6 ± 6.1 (n = 4)	Present study
Single ice crystal	13–18.5			9
Single ice crystal	2.8–17.5			3
Sea ice	3–100	7.9–22.2		24
Sea ice		0.75–3.31		2
Sea ice		3–13		1

We have repeatedly found that the mean stress during the fluctuations is approximately 75% of the maximum stress. Since it is operationally simpler, we define strength based on the maximum stress, although the fluctuating stress at, on average, 75% of that level might be viewed as more representative.

This view of the observations motivates the extraction of two representative parameters from the experimental results: E, the elastic modulus (from the initial portion of the curve, or between stress drops) and σ_{max}, the maximum strength of the frozen tissue, points M in Figs. 4 and 5. These are compared with data from sea ice and single ice crystals in Table 1. The elasticity modulus was measured a few times for each sample, before and during the stress drops, and therefore the group size for the elasticity modulus in Table 1 is larger than for the maximal strength (only one value of maximal strength can be obtained from each sample). The mechanical properties of sea ice have been widely studied for sea transportation (24); their strength and elasticity modulus have been found from standard compression tests (1, 2). The elastic modulus for single ice crystals were measured with ultrasonic techniques (3, 9). It seems worthwhile to compare biological tissues with sea ice because both have high saline content and since the bulk of biological tissue is water.

The elastic moduli of frozen tissues from rabbit liver, kidney, and brain fall within the wide range of values reported for sea ice and are rather close to the elastic modulus of single ice crystals. The maximum strength appears to be up to one order of magnitude higher than the yield strength of sea ice. These large differences cannot be explained by the different definitions for strength, where the maximal strength of sea ice is less than 1.5 times the yield strength (24). The large differences may be explained by the contribution of the extracellular matrix and the biological fibers to the strength of the frozen tissue (making it a composite material), which are absent from sea ice. One may speculate that the strength under tensile stress (shown earlier to be relevant to cryoprocedures) would be no more than, and possibly much less than, the compressive strength. This is based on the interpretation of stress drops as signaling microcrack formation and on the relatively weak response in tension typical of such brittle materials.

Two additional observations were made during the experimental work, which are not quantified at this stage: (i) The frozen brain tissue was found to be much less resistant to

impact than the other frozen tissues. (ii) Samples taken from the cortex of the kidney were found to be stronger and stiffer than samples taken from the medulla.

The liver, kidney, and brain have different strengths and stiffness, with the frozen kidney tissue having higher values and the frozen brain tissue having lower values. It was demonstrated by Rabin and Steif (19) that the *ratio* of yield strength to stiffness, σ_y/E, is a critical parameter in the elastic–perfectly plastic thermal stress problem. Although there are significant differences in the mechanical properties among the frozen liver, kidney, and brain, the ratio $\sigma_{y,ave}/E$ was found to be 2.7×10^{-3}, 4.4×10^{-3}, and 2.3×10^{-3} for the liver, kidney, and brain, respectively; where $\sigma_{y,ave}$ is defined here as 75% of σ_{max}, as discussed above.

It was suggested by Gao *et al.* (8) that the thermal expansion coefficient is the dominate parameter that characterizes the phenomenon of fracture in the frozen material. Gao *et al.* have studied the effect of glycerol, as a cryoprotectant, on the thermal expansion coefficient. Here we claim that the tendency to fracture depends on the strength (or strength-to-stiffness ratio) which limits the level of stresses, in addition to the thermal expansion coefficient which drives the thermal stresses. For example, a frozen material with a higher strength-to-stiffness ratio will be able to withstand higher strains due to thermal expansion before the first fracture appears, for a given arbitrary temperature gradient. It follows that the influence of cryoprotectants, or cryosensitizers, on the strength to stiffness ratio should also be studied in order to gain a better control on cryopreservation or cryodestruction processes.

It is known that the freezing temperature of water decreases as the pressure increases, above some extreme critical pressure. For example, the freezing temperature of water at 100 MPa is −9°C (12). Since the compression tests in this study were performed at the liquid nitrogen boiling temperature, i.e., −196°C, the effect of a pressure-dependent freezing temperature should not influence the results. However, this effect might be taken in account in future mathematical analyses, in regions where high stresses are developed at relatively high temperatures.

SUMMARY AND CONCLUSIONS

A pilot study of the mechanical response of frozen soft biological tissues to an external load in compression is presented. The main concept in this study is that the mechanical load due to the constrained contraction of the frozen tissue, i.e., due to temperature variations within the frozen region, can be simulated by an external mechanical load which is applied directly to the frozen tissue, which is held at a uniform temperature. The rationale for this concept is well established in the study of deformable bodies: the deformations associated with stresses are not dependent on the origin of the stress. The mechanical properties under study in the present work are the compressive strength and the elastic modulus.

A new load chamber for measuring the stress–strain relationship of frozen biological tissues in cryogenic temperature range was designed and constructed. The load chamber can fit into a standard mechanical testing apparatus. A new technique for processing the fresh soft biological tissue into a cylindrical frozen sample for a compression test is introduced.

Experimental data of the strength and elastic modulus of rabbit liver, kidney, and brain in a cryogenic temperature range are presented. Comparing with available data from the literature, the elastic modulus of frozen tissues was found to be within the wide range of elastic modulus reported for sea ice. Liver and brain tissues were found to be within the wide range of elastic moduli of single ice crystals, while kidney tissues were found to be about 20% stiffer than the upper end of the single ice crystals range. The maximal strength of the frozen tissues appears to be up to one order of magnitude higher than the yield strength of sea ice. The ratio of an aver-

age yield strength to stiffness of different frozen tissues, however, was found to be approximately 3×10^{-3}. Due to the dense capillary network and the high blood content, the mechanical properties of liver are expected to be similar of those of the blood. The mechanical properties of frozen blood, as a function of the cooling protocol, are now under experimental study.

A unique response of frozen biological tissues to compression was observed. We have found elastic behavior up to rather small strains, on the order of 0.005, and a sawtooth pattern of stress thereafter featuring a series of sudden stress drops followed by a linear return to a roughly constant upper level of stress. It is suggested that the stress drops are associated with the formation of microcracks which steadily accumulate until final failure. The highly heterogeneous nature of this material may allow such cracks to appear, but not to propagate. Complete unloading leaves the material with a permanent plastic strain; continued microcracking only resumes when the stress is returned to the previous level at which microcracking occurred. The jagged nature of the curves notwithstanding, it appears that the mechanical response of frozen tissues can usefully be idealized by elastic–perfectly plastic models.

It is argued in the present study that the relationship between the thermal expansion coefficient and the strength-to-stiffness ratio is the dominant factor of fractures appearance, since it represents the relationship between the driven source and the consequential mechanical response in the frozen material. It follows that the influence of cryoprotectants, or cryosensitizers, on the strength-to-stiffness ratio should be studied in order to gain a better control on cryopreservation or cryodestruction processes.

ACKNOWLEDGMENTS

This research was supported in part by Allegheny-Singer Research Institute (96-026-2P), Pittsburgh, Pennsylvania. The authors thank Mr. John W. Zinn, a graduate student at the Department of Mechanical Engineering at Carnegie Mellon University, for his excellent assistance in mechanical testing. The authors also thank Dr. Tommy Shih, a research associate at the Department of Neurosurgery at Allegheny General Hospital, for his special assistance in extracting the brain tissues.

REFERENCES

1. Brown, R. L. An evaluation of the rheological properties of columnar ridge sea ice. *In* ''Ice Technology'' (Murthy, T. K. S., Connor, J. J., and Brebbia, C. A., Eds.), Proceedings, 1st International Conference, Cambridge, MA, Springer-Verlag, Berlin, 1986.
2. Christensen, F. T. Sea ice strength measurements from the inner Danish waters in early 1985. *In* ''Ice Technology'' (Murthy, T. K. S., Connor, J. J., and Brebbia, C. A., Eds.), Proceedings, 1st International Conference, Cambridge, MA, Springer-Verlag, Berlin, 1986.
3. Dantl, G. Elastic moduli of ice. *In* ''Physics of Ice'' (Riehl, N., Bullemer, B., and Engelhardt, H., Eds.), pp. 223–230. Plenum, New York, 1969.
4. Fahy, G. M. The relevance of cryoprotectant ''toxicity'' to cryobiology. *Cryobiology* **23,** 1–13 (1986).
5. Fahy, G. M., Saur, J., and Williams, R. J. Physical problems with the vitrification of large biological systems. *Cryobiology* **27,** 492–510 (1990).
6. Gage, A. A. Critical temperature for skin necrosis in experimental cryosurgery. *Cryobiology* **19,** 273–281 (1982).
7. Gage, A. A., Guest, K., Montes, M., Garuna, J. A., and Whalen, D. A., Jr. Effect of varying freezing and thawing rates in experimental cryosurgery. *Cryobiology* **22,** 175–182 (1985).
8. Gao, D. Y., Lin, S., Watson, P. F., and Critser, J. K. Fracture phenomena in an isotonic salt solution during freezing and their elimination using glycerol. *Cryobiology* **32,** 270–284 (1995).
9. Helmreich, D. Elastic anomalies of ice at low temperatures. *In* ''Physics of Ice'' (Riehl, N., Bullemer, B., and Engelhardt, H., Eds.), pp. 231–238. Plenum, New York, 1969.
10. Hunt, C. J., Song, Y. C., Bateson, A. J., and Pegg, E. D. Fractures in cryopreserved arteries. *Cryobiology* **31,** 506–515 (1994).
11. Ishiguro, H., and Rubinsky, B. Mechanical interaction between ice crystals and red blood cells during directional solidification. *Cryobiology* **31,** 483–500 (1994).
12. Lide, D. R. (Ed.) ''Handbook of Chemistry and Physics,'' 75th ed., pp. 6–53. CRC Press, Boca Raton, FL, 1995.
13. Mazur, P. Kinetics of water loss from cells at subzero temperatures and the likelihood of intracellular freezing. *J. Gen. Phys.* **44,** 347–369 (1963).
14. Mazur, P., Leibo, S., and Chu, E. H. Y. A two-factor

hypothesis of freezing injury. *Exp. Cell Res.* **71,** 345–355 (1972).

15. McGrath, J. J. Low temperature injury processes. *In* ''Advances in Bioheat and Mass Transfer'' (R. B. Roemer, Ed.), Vol. 268, pp. 125–132. ASME HTD, 1993.
16. Meryman, H. T. Freezing injury and its prevention in living cells. *Annu. Rev. Biophys. Bioeng.* **3,** 341–363 (1974).
17. Miller, R. H., and Mazur, P. Survival of frozen–thawed human red cells as a function of cooling and warming velocities. *Cryobiology* **13,** 404–414 (1976).
18. Paterson, M. S. ''Experimental Rock Deformation—The Brittle Field.'' Springer-Verlag, Berlin, 1978.
19. Rabin, Y., and Steif, P. Analysis of thermal stresses around cryosurgical probe. *Cryobiology* **33,** 276–290 (1996).
20. Rand, R. W., Rand, R. P., Eggerding, F. A., Field, M., Denbesten, L., King, W., and Camici, S. Cryolumpectomy for breast cancer: an experimental study. *Cryobiology* **22,** 307–318 (1985).
21. Rubinsky, B., Cravalho, E. G., and Mikic, B. Thermal stress in frozen organs. *Cryobiology* **17,** 66–73 (1980).
22. Shlafer, M. Drugs that modify cellular responses to low temperature (cryoprotectants): A pharmacological perspective of preserving biological systems by freezing. *Fed. Proc.* **36**(12), 2590–2594 (1977).
23. Smith, J. J., and Fraser, J. An estimation of tissue damage and thermal history in cryolesion. *Cryobiology* **11,** 139–147 (1974).
24. Weeks, W., and Assur, A. ''The Mechanical Properties of Sea Ice.'' Cold Regions Research & Engineering Laboratory, U.S. Army, Hanover, NH, 1967.